Industrial Crops & Products 178 (2022) 114617

Contents lists available at ScienceDirect

Industrial Crops & Products

journal homepage: www.elsevier.com/locate/indcrop

What leads to rubber leaf senescence in the northern edge of the Asian tropics?

Yaoliang Chen [a,b,c], Shusen Wang [d], Ruiwu Zhou [e], Palingamoorthy Gnanamoorthy [f], Qinghai Song [f,*], Houbing Chen [a,c]

[a] *State Key Laboratory for Subtropical Mountain Ecology of the Ministry of Science and Technology and Fujian Province, Fujian Normal University, Fuzhou 350 007, China*
[b] *Fujian Provincial Key Laboratory for Subtropical Resources and Environment, Fujian Normal University, Fuzhou 350 007, China*
[c] *School of Geographical Sciences, Fujian Normal University, Fuzhou 350 007, China*
[d] *Canada Centre for Remote Sensing, Natural Resources Canada, Ottawa K1A 0E4, Canada*
[e] *School of Geography and Land Engineering, Yuxi Normal University, Yuxi 653 199, China*
[f] *CAS Key Laboratory of Tropical Forest Ecology, Xishuangbanna Tropical Botanical Garden, Chinese Academy of Sciences, Menglun 666 303, China*

ARTICLE INFO

Keywords:
Rubber tree
Leaf senescence
Phenology
Climate factors

ABSTRACT

The rubber tree (*Hevea brasiliensis*) belongs to the evergreen broadleaved species in its native ranges, but it has a concentrated leaf senescence period after it was introduced to the Asian tropics. The mechanism behind the leaf senescence is still unclear. Models for predicting leaf senescence dates of this introduced tree have been rarely explored. This study proposed a series of models to identify the main abiotic drivers for the rubber leaf senescence which include temperature, daylength, and water stress. Model tests using data observed from the rubber plantations over the Xishuangbanna region in China show that: (1) Low temperature or cold stress played more critical roles than water stress and daylength in driving rubber leaf senescence. While models using air temperature and soil temperature showed similar performance, the former was recommended for leaf senescence modelling as it is easy to obtain. (2) The root mean square error of all the proposed models was significantly lower than that of the null model which used the mean date of leaf senescence over the study years, indicating the ability of our proposed models in predicting rubber leaf senescence dates. However, no significant differences were found among the proposed models. The thermal time senescence model was recommended for leaf senescence modelling as it is easy to implement. This study helps to better understand the driving mechanism of rubber leaf senescence.

1. Introduction

Hevea brasiliensis (the rubber tree) is a species native to the Amazon tropical regions (Carr, 2012; George et al., 2009; Priyadarshan, 2017), but it has witnessed an unprecedented spread to Africa, Southeast Asia and tropical areas of China because of the huge demand for natural rubber in the international market (Fox and Castella, 2013; Liu et al., 2016). It originally belongs to the evergreen broadleaved species in its native ranges; however, it has a concentrated leaf senescence period (up to 4 weeks) after it was introduced to the Asian tropics (Chen and Cao, 2015; Li et al., 2016). Identifying the reasons for this kind of phenology change is crucial for improving our knowledge of the interaction between climate and ecosystems. However, to date, the mechanism of intense defoliation for these introduced rubber trees is still unclear. Besides, models for predicting leaf senescence dates of this introduced plantations have been rarely explored. Therefore, this study aims to develop suitable rubber leaf senescence predicting models and to identify the driver of rubber tree senescence in the northern edge of the Asian tropics.

Sound knowledge of drivers and mechanisms on phenology is necessary for accurately predicting plant phenology (Piao et al., 2006, 2019; Ge et al., 2015; Hufkens et al., 2018). Leaf senescence is found to be largely regulated by age and abiotic and biotic factors (Koyama, 2014). One of the most important biotic factor is the plant hormone

---

* Corresponding author.

E-mail addresses: chenyl@fjnu.edu.cn (Y. Chen), shusen.wang@canada.ca (S. Wang), zhouruiwu@yxnu.edu.cn (R. Zhou), gnanamoorthy@xtbg.ac.cn (P. Gnanamoorthy), sqh@xtbg.ac.cn (Q. Song), chenhb1999@gmail.com (H. Chen).

https://doi.org/10.1016/j.indcrop.2022.114617
Received 27 November 2021; Received in revised form 19 January 2022; Accepted 25 January 2022

ethylene (Lürssen, 1991; Lee et al., 2021). The ethylene is found to be strongly influenced by abiotic factors to accelerate or delay leaf senescence, but its response to abiotic stress is rather complex (Zhao et al., 2014; Kazan, 2015; Lee et al., 2021). Three abiotic factors, including temperature (T), daylength (D) and water availability (or water stress; W) are commonly considered the key factors that control vegetation evolution over time (Piao et al., 2019). Temperature is generally regarded as the main driver of plant phenology, especially for spring phenology (Caffarra et al., 2011; Chuine, 2010; Cleland et al., 2007; Picornell et al., 2019; Recio et al., 2018). Warming leads to earlier springs and later autumns while cooling delays the arrival of spring and advances the arrival of autumn (Menzel et al., 2006). Accumulated low temperature (chilling) is broadly understood to be an independent prerequisite for breaking the endodormancy (the first stage of plant dormancy, a state of inactivity mediated by factors inside the bud) of leaf budburst. Subsequently, a certain accumulation of high temperature (forcing) is generally needed to break the ecodormancy (the second stage of plant dormancy, a state of inactivity imposed by unfavorable environmental conditions at otherwise full preparedness for advancing seasonal development) of leaf budburst (Basler, 2016; Chuine, 2000; Cook et al., 2012; Delpierre et al., 2016; Hanninen, 2016; Lang, 1987). Daylength is able to regulate leaf senescence in some vegetation species, such as defoliation of European aspens (Cook et al., 2012; Fracheboud et al., 2009) and coloring of herbaceous plants in the Inner Mongolian steppe (Tao et al., 2020) and of 27 woody and herbaceous species in the Qinghai–Tibetan Plateau (Lang et al., 2019). The effect of daylength on leaf budburst is not as clear as it is for leaf senescence (Chuine, 2010; Körner and Basler, 2010; Piao et al., 2019), although some studies have found its dominant control on the leaf-out of temperate deciduous trees (Fu et al., 2019) and its interaction with temperature in co-regulating the timing of leaf budburst (Basler and Koerner, 2014; Fu et al., 2015; Way and Montgomery, 2015). Plant phenology in most temperate arid and tropical dry regions is strongly influenced by water availability, such as precipitation, soil moisture and atmosphere vapor pressure deficit (Broadhead et al., 2003; Di Lucchio et al., 2018; Mendez-Alonzo et al., 2013; Seghieri et al., 2012; Semerci et al., 2020), although it is not supported as the main environmental driver of leaf flushing in woody species in central Sahel and southern Africa (Ryan et al., 2017; Seghieri et al., 2012; Tian et al., 2018). Other factors such as wind speed, radiation, may play key roles in phenology. For example, it was found that decline in winds delayed leaf senescence (Wu et al., 2021). Overall, more and more consensus has been reached on the mechanisms of spring phenology, and the drivers tend to be species-specific (Hufkens et al., 2018; Jeong et al., 2012; Migliavacca et al., 2012; Richardson et al., 2013). However, knowledge of environmental drivers for leaf senescence still remains largely unclear (Jeong and Medvigy, 2014; Keenan and Richardson, 2015; Klosterman et al., 2014; Piao et al., 2019).

Over the past decades, numerous models have been developed to predict plant phenology (Basler, 2016; Hufkens et al., 2018). As a result of the lack of experimental evidence regarding involved factors and the poorly understood mechanisms, to date, models for predicting leaf senescence are limited compared with spring phenology models (Jolly et al., 2005; Piao et al., 2019). Current leaf senescence models are usually based on either specific temperature or daylength threshold for certain cooling degree-days (CDDs), which is similar to growing degree-days (GDDs) in many spring phenology models (Delpierre et al., 2009; Keenan and Richardson, 2015). However, almost all these leaf senescence models are developed for temperate ecosystems wherein phenological phase transitions are obvious. Models of leaf senescence are rarely explored for subtropical and tropical ecosystems, especially for introduced rubber trees.

The introduced rubber trees have a concentrated defoliation period lasting 2–4 weeks in the northern edge of the Asian tropics (Carr, 2012; Li et al., 2016; Priyadarshan, 2017). Though some studies have explored the mechanisms of intense defoliation for rubber trees through different methods, no consensus has been reached so far. For example, Liu et al. (2014) suggested rubber leaf senescence is mainly a result of drought stress as root water uptake was found to be transferred from shadow soil layer to deep soil layer during the period of defoliation. Chen et al. (2010) also supported this result, but they suggested water conductivity of xylem catheter is low when drought stress occurs and leaves start to senescence. Conversely, Lin et al. (2018) suggested that low temperature is more relevant to dense defoliation than drought stress, and they found rubber leaves start to senescence when a certain accumulated low temperature (<10 °C) is reached. Guardiola-Claramonte et al. (2010) suggested that rubber leaf senescence is accounted for not by a single factor but by multiple factors, including temperature, water availability and daylength. These inconsistent conclusions have resulted from a lack of comprehensive consideration of potential driving factors based on long-term phenology observations. Taking a tropical region of China as the study location, this study aimed to (1) identify the main factors driving rubber leaf senescence; and (2) develop reliable models to improve rubber senescence prediction.

2. Materials and methods

2.1. Study area

The study site is located in the Xishuangbanna Tropical Botanical Garden (XTBG), Chinese Academy of Sciences, Yunnan Province, Southwest China. Rubber trees were induced in the year of 1987 and planted in a small catchment with spacing of 2.1 × 4.0 m (around 370 trees per ha) in an area of around 0.19 km^2 after completely cutting the primary forest (Liu et al., 2014). The altitude of this catchment is in the range of 560–730 m a.s.l. with a mean slope of 16°. Belonging to a tropical humid and monsoon climate, the study area has two obvious seasons: rainy season from May to October, and dry season from November to April. Annual mean precipitation based on multiyear observations was around 1490 mm with most occurring during the rainy season (Lin et al., 2018). The average annual temperature was around 21.7 °C, with maximum daily average temperature of 29.4 °C and minimum daily average temperature of 7.2 °C. The mean diameter at breast height was 22 cm, and the canopy height of the rubber plantation was around 20–30 m. Roots of rubber trees can reach a maximum depth of 2 m in soil with a clay–loam texture (around 42% coarse sand, 34% silt and 24% clay). Rubber trees have an intense defoliation period lasting 2–4 weeks during the dry season, commonly occurring in January and February (Guardiola-Claramonte et al., 2010). Leaf flushing usually happens during the weeks before the arrival of the rainy season.

2.2. Phenological observations

In this study, the defoliation start date was used as the proxy of leaf senescence. Time series records of rubber tree defoliation start date were obtained from two sources for different periods: (1) start dates from 1994 to 2008 (observations of 1996, 1998–2000 were missing) were downloaded from National Earth System Science Data Sharing Infrastructure, National Science & Technology Infrastructure of China (http://www.geodata.cn; accessed February 20, 2020). These phenology datasets were recorded by the Chinese Phenological Observation Network (CPON), which was established in 1963 and administrated by the Institute of Geographical Sciences and Natural Resources Research (IGSNRR), Chinese Academy of Sciences (CAS) (Ge et al., 2015); (2) start dates for the years 2009–2016 were recorded by manual observation by the Gardening and Horticulture Department of XTBG. Both these phenological observations were carried out in XTBG (21°56′N, 101°15′E, 580 m a.s.l.) by professionals at weather stations according to uniform observation criteria (Wan and Liu, 1979).

2.3. Climate data

Three categories of factors, including temperature, water availability and daylength, were selected in this study. Temperature factors include daily average air temperature (T_{avg}), daily minimum air temperature (T_{min}), daily average soil temperature at depth of 5 cm (T_{s5}) and daily average soil temperature at depth of 20 cm (T_{s20}). Water availability factors include atmosphere vapor pressure deficit (W_{VPD}) and soil moisture at 100 cm (W_{soil}). Daylength (D) is calculated as the duration when solar elevation angle is above 0 °. Dataset of T_{avg}, T_{min}, T_{s5}, T_{s20}, W_{VPD}, and D for the period 1993–2016 were obtained from National Forest Ecosystem Research Station at Xishuangbanna (http://bnf.cern.ac.cn/meta/metaData). Limited W_{soil} from 2010 to 2016 was also obtained from National Forest Ecosystem Research Station. W_{soil} data for the other years (1993–2009) were derived from Global Land Data Assimilation System (GLDAS) Catchment Land Surface Model (CLSM) L4 daily 0.25 × 0.25° V2.0 (GLDAS_CLSM025_D). The version 2.0 of GLDAS is forced entirely with the Princeton meteorological forcing input data and provides a temporally consistent series from 1948 through 2014. The W_{soil} data from GLDAS has been corrected by using the linear correlation between observed W_{soil} and GLDAS W_{soil} during the same period (2010–2014). All the Pearson correlation coefficients between GLDAS and observed daily soil moisture in each overlapped year (2010–2014) exceeds 0.90, indicating a good consistence between this two datasets. Statistics of all the seven factors during pre-leaf senescence period from September 23 to the end of next March over the 19 study years is provided in Table 1.

2.4. *Model development and implementation*

There is no consensus on the formulation of leaf senescence for tropical deciduous trees. Thus, in this study, we developed a family of rubber leaf senescence models (Table 2) based on existing spring phenology models (i.e., one forcing model: thermal time model (TT) (Cannell and Smith, 1983); and four chilling-forcing models: unified model (UN) (Chuine, 2000), sequential model (SQ) (Hänninen, 1990), alternating model (AT) (Cannell and Smith, 1983) and parallel model (PA) (Landsberg, 1974)). Detailed formulations of these spring models can be found in previous literatures (Basler, 2016; Hufkens et al., 2018). Detailed formulations of our rubber leaf senescence models are provided in Table 3. An explicit description of response differences between the newly developed rubber leaf senescence models and spring phenology models is shown in Fig. 1, followed by subsections providing the detailed descriptions.

2.4.1. *Development of thermal time model for leaf senescence*

Thermal time model for leaf senescence was constructed by developing a decreasing degree-day (DDD) response (TTF model in Fig. 1a and Table 3) or decreasing sigmoid response (TTFs model in Fig. 1b and Table 3) between energy (sum of environmental factor below a given threshold) and the senescence state. The leaf senescence event occurs when forcing state with a certain accumulated energy is reached. It is reasonable to assume a decreasing response of environmental factors such as temperature, daylength and soil moisture to leaf senescence as accumulation of cold temperatures, short daylength or low soil moisture have been highlighted as strong predictors of autumn senescence (Bréda et al., 2006; Dragoni et al., 2011; Estrella and Menzel, 2006; Keskitalo et al., 2005). It is worthy noting that the leaf senescence response of forcing state to energy (Figs. 1a and 1b) is totally opposite to the spring phenology response (Fig. 1a' and 1b').

Table 1
Statistics of all three category factors (temperature, daylength and water availability) during pre-leaf senescence period from September 23 to the end of next March over the 19 study years.

	T_{avg} (°C)	T_{min} (°C)	T_{s5} (°C)	T_{s20} (°C)	D (h)	W_{VPD} (pa)	W_{soil} (m^3/m^3)
Max	26.90	23.70	31.70	31.10	17.40	771.57	0.46
Min	7.40	4.40	13.60	16.20	0.00	0.00	0.10
Mean	19.12	15.06	22.79	23.45	4.90	303.59	0.25
Std	3.22	3.91	3.15	2.98	2.42	124.01	0.07

Note: T_{avg}, T_{min}, T_{s5}, T_{s20}, D, W_{VPD} and W_{soil} represent daily average temperature, daily minimum temperature, soil temperature at depth of 5 cm, soil temperature at depth of 20 cm, daylength, vapor pressure deficit and soil moisture at depth of 100 cm, respectively.

Table 2
Overview of proposed leaf senescence models in this study.

Model name	Pre-stress response	Forcing response	Criteria for leaf senescence	Number of parameters
Thermal time senescence model with DDD forcing function (TTF)	None	DDD response	Accumulated forcing energy lower than a certain threshold	3
Thermal time senescence model with sigmoid forcing function (TTFs)	None	Sigmoid response		4
Sequential senescence model with trapezoid response of pre-stress (SQF)	Trapezoid response	DDD subsequently occurred with pre-stress state		8
Sequential senescence model with sigmoid response of pre-stress (SQFs)	Sigmoid response			8
Parallel senescence model with trapezoid response of pre-stress (PAF)	Trapezoid response	DDD synchronously occurred with pre-stress state		8
Parallel senescence model with sigmoid response of pre-stress (PAFs)	Sigmoid response			8
Alternating senescence model (ATF)	Binary response	DDD	Accumulated forcing energy reaches accumulated pre-stress energy	5
Unified senescence model (UNF)	Bell response	DDD	Accumulated forcing energy reaches a value related to accumulated pre-stress energy	9

Note: DDD, Decreasing degree-day.

2.4.2. *Development of sequential model, parallel model, alternative model and unified model for leaf senescence*

In this study, we assumed there is a pre-stress state before leaf senescence forcing state to construct sequential rubber leaf senescence (SQF) model, parallel rubber leaf senescence (PAF) model, alternating rubber leaf senescence (ATF) model and unified rubber leaf senescence (UNF) model. This is because plants were assumed to exhibit similar pre-

Table 3

Driver response functions and structures of pre-stress/forcing-based leaf senescence models.

Pre-stress/forcing response functions to leaf senescence			
Trapezoid response	$r_t(X_i)=\left\{\begin{array}{c} X_{opt} \leq X_i < X_{max} : X_i - X_{max} \\ X_{min} \leq X_i < X_{opt} : X_{opt} - X_{max} \\ X_i > X_{max} \text{ or } X_i < X_{min} \ :0 \end{array}\right\}$	DDD response	$r_d(X_i)=\left\{\begin{array}{c} X_i \leq X_{base}: X_i - X_{base} \\ X_i > X_{base}:0 \end{array}\right\}$
Valley-shaped response	$r_v(X_i)= -\frac{1}{1+e^{(a*(X_i-c)^2+b(X_i-c))}}$	Sigmoid response (SF)	$r_s(X_i)= -\frac{1}{1+e^{b(X_i-c)}}$
Binary 0/1 response	$r_b=\left\{\begin{array}{ll} 0 & X_i > X_{base} \\ 1 & X_i \leq X_{base} \end{array}\right\}$		
Leaf senescence models			
State of pre-stress	$\boldsymbol{S_{prs}} = \sum_{i=t_0}^{n} \boldsymbol{R_{prs}}$	State of forcing	$\boldsymbol{S_{frc}} = \sum_{i=t_0}^{n} \boldsymbol{R_{frc}}$
		Criteria for bud burst	$\boldsymbol{S_{frc} \geq F_{crit}}$
Thermal time senescence model with DDD forcing function (TTF)	$R_{frc}=r_d$	Thermal time senescence model with sigmoid forcing function (TTFs)	$R_{frc}=r_s$
Sequential senescence model with trapezoid response of pre-stress (SQF)	$R_{prs}=r_t R_{frc}= kr_d k = \left\{\begin{array}{l} S_{prs} > P_{req} : 0 \\ S_{prs} \leq P_{req} : 1 \end{array}\right\}$	Sequential senescence model with sigmoid response of pre-stress (SQFs)	$R_{prs}=r_s R_{frc}= kr_d k = \left\{\begin{array}{l} S_{prs} > P_{req} : 0 \\ S_{prs} \leq P_{req} : 1 \end{array}\right\}$
Parallel senescence model with trapezoid response of pre-stress (PAF)	$R_{prs}=r_t R_{prs}= kr_d k = \left\{\begin{array}{c} S_{prs} > P_{req} : P_{ini} + S_{prs}\frac{1-P_{ini}}{P_{req}} \\ S_{prs} \leq P_{req} : 1 \end{array}\right\}$	Parallel senescence model with sigmoid response of pre-stress (PAFs)	$R_{prs}=r_s R_{frc}= kr_d k = \left\{\begin{array}{c} S_{prs} > P_{req} : P_{ini} + S_{prs}\frac{1-P_{ini}}{P_{req}} \\ S_{prs} \leq P_{req} : \quad 1 \end{array}\right\}$
Unified senescence model (UNF)	$R_{prs}=r_v k = \left\{\begin{array}{ll} S_{prs} > P_{req} : & 0 \\ S_{prs} \leq P_{req} : & 1 \end{array}\right\} R_{frc}= kr_d F_{crit}=we^{fS_{prs}}$	Alternating senescence model (ATF)	$R_{prs} = r_b R_{frc}=r_d F_{crit}=a+be^{cS_{prs}}$

Note: The r_t, r_d, r_v, r_s and r_b represent the trapezoid, decreasing-degree-day, valley-shaped, sigmoid, and binary response respectively. The driver X_i in the formulations refers to any factor from daily mean temperature, daily minimum temperature, soil temperature at depth of 5 cm, at depth of 20 cm, daylength, and vapor pressure deficit. The X_{min}, X_{base}, and X_{max} represent the minimum value, baseline threshold and maximum value of driver factor X_i respectively. The S_{prs} and S_{frc} represent the state value of pre-stress and forcing. t_0, F_{crit} and P_{req} represent the start of baseline date, the criteria for forcing state and the request of pre-stress units, respectively. a, b, c, w, f, P_{ini} are parameters which need to be fixed in the simulation. DDD represents decreasing degree-day.

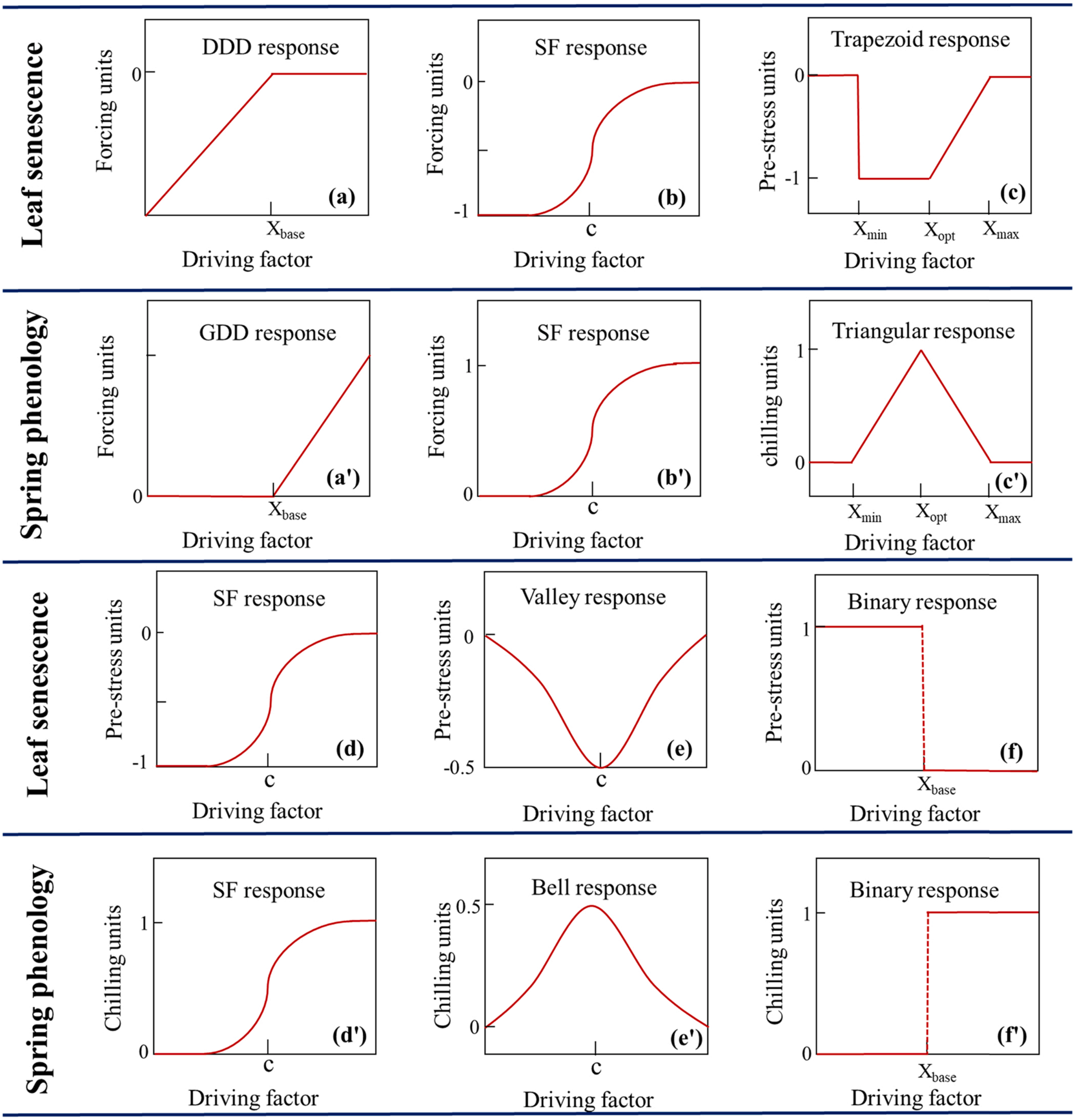

Fig. 1. Response differences in pre-stress/chilling and forcing states between the proposed leaf senescence models (a–f) and their corresponding derived spring phenology models (a'–f'). Detailed equations of leaf senescence models are provided in Table 3. Detailed equations of spring phenology models can be found in Basler (2016) and Hufkens et al. (2018). The X_{min}, X_{opt}, and X_{max} represent the minimum value, optimal value and maximum value of driver factor respectively. c represents a parameter which need to be fixed in the simulation.

stress (i.e., pre-cooling) responses to these unfavorable stresses like drought and coldness before leaf senescence (Kramer, 1940; Lin et al., 2018). Formulations of these proposed models are provided in Table 3. A trapezoid function of pre-stress response of SQF and PAF for leaf senescence (Fig. 1c) was developed and it is different from the triangle functions in SQ and PA for spring phenology (Fig. 1c'). This is because it is more reasonable if the pre-stress units are held at maximum rather than decreasing after the optimum value is reached in the leaf senescence process. Sigmoid function was induced as alternative choice for pre-stress response to construct two other leaf senescence models: SQFs and PAFs. Sigmoid responses in leaf senescence (Fig. 1d) and spring phenology (Fig. 1d') are very similar except that they have opposite units. Alternating leaf senescence (ATF) model and unified leaf senescence model (UNF) were also constructed. A binary function (either 0 or 1) (Fig. 1f) to reflect the response of pre-stress was used in the ATF model. This is similar to a responding flipped binary function (also either 0 or 1) in the chilling process of AT model for spring phenology (Fig. 1f'). We adopt a valley function as the pre-stress response for leaf senescence in UNF model (Fig. 1e) comparing with the bell function of UN model for spring phenology (Fig. 1e').

2.5. Model implementation and parameterization

In order to compare the results of different factors and different leaf senescence models, a total of 56 scenarios comprised of the aforementioned seven factors (T_{avg}, T_{min}, T_{s5}, T_{s20}, D, W_{VPD} and W_{soil}) and eight models (i.e., TTF, TTFs, SQF, SQFs, PAF, PAFs, ATF and UNF) were implemented. All the rubber leaf senescence models mentioned earlier were developed based on PHENOR R package, which is an integrated spring phenology modeling framework developed by Hufkens et al. (2018).

As rubber leaves generally start to fall around January, we set the phenological year as starting on September 23 and ending on the next September 22. September 23 was set as the beginning date because it is autumnal equinox and a transition date from summer to autumn. The parameters and their quantities vary with different models (Table 1). Some parameters, such as starting day of energy sum calculation, base value of environmental factor, state of forcing and state of pre-stress, coexist in most models (Table 1). All the parameters were initialized within a reasonable range before model simulation. The final value of each parameter was fitted using the simulated annealing algorithm of Metropolis (Chuine et al., 1998). Simulated annealing refers to an analogy with a thermodynamic principle on the way metals cool and anneal or liquids freeze and crystallize. The detailed principle of this algorithm can be found in Chuine et al. (1998).

2.6. Model calibration and validation

As the observed leaf senescence dates were limited, leave-one-out cross-validation over the 19-year observation period for each factor was used to calibrate and assess the general performance of the proposed models. Specifically, the observed samples were first divided into 19 folds: 18 were used for model calibration and 1 for model validation. This process was iterated 19 times to make sure all observations were used in model building at least once. Then, 10 repeats for the leave-one-out process were implemented to obtain enough results for each calibrated model. Root mean square error (RMSE) was used to determine the best calibrated model and assess the prediction of best model. Potential optimal models and factors were selected according to the performance of each model and factor. Then, the final parameters of each selected model were derived from datasets of all the 19 years.

2.7. Statistics for comparison

First, the model performance was compared using an ANOVA on the RMSE of each environmental factor. Then, comparison for all the models was conducted based on the determined driving factors from the factor comparison result. Post-hoc Tukey HSD test was used to identify performance differences among factors and models.

3. Results

3.1. Phenological observations – general remarks

Over the 19 years, the rubber leaf senescence start date ranged from day of year (DOY) 355 (December 20) to 38 (February 7) with a standard variation of 12.3 days (Fig. 2). The mean rubber senescence start date was found to be DOY 15.3. There is a trend of a 0.86-day delay per year in leaf senescence start date with a significant level of $\alpha = 0.05$. It is worth noting that trends in the first 10 years and the last 10 years are greatly different. The first 10 years showed a more stable trend compared with the large variation seen during the last 10 years. This is mainly because of a more extensive climate variation in the last 10 years than during the former 10 years in the study area.

3.2. Performance of different climatic factors

Comparison of RMSE of predicted leaf senescence date for each climate factor (Fig. 3) shows the RMSE of temperature-based (i.e., T_{avg}, T_{min}, T_{s5} and T_{s20}) models was generally lower than that of models derived using other factors, indicating that temperature-based models outperform daylength and water availability factors regardless of the type of model used. For example, the mean RMSEs of models based on T_{avg}, T_{min}, T_{s5} and T_{s20} were around 6.7–10.4 days (Fig. 3), which were about 1–6 days lower than those of models based on D, W_{VPD} and W_{soil} (Fig. 4). This implies that rubber leaf senescence was most likely driven by temperature factors rather than other environmental factors such as drought. Among all the factors, T_{s20} performed best with a mean RMSE of 6.7 days and a minimum RMSE of 5.5 days (SQFs model). The mean

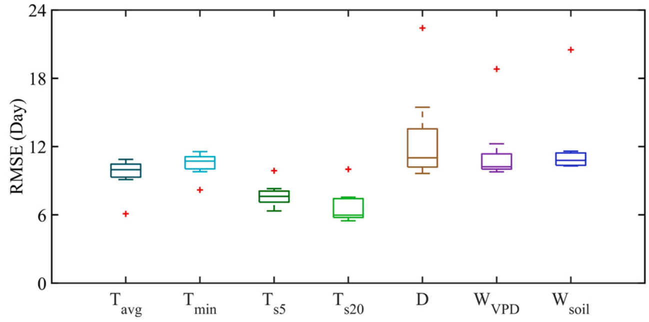

Fig. 3. Boxplot of different factors for comparing their effects on rubber leaf senescence.

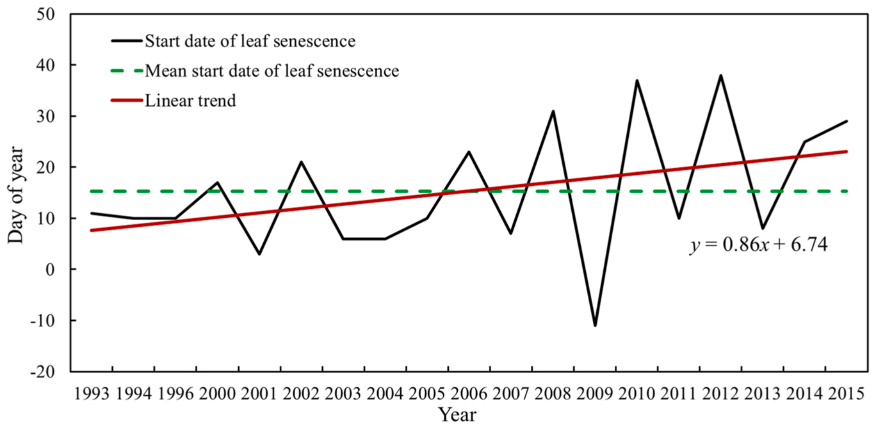

Fig. 2. Observed rubber leaf senescence start date (black line) as day of year from 1993 to 2016. The dashed green line is the mean and the linear red line is the trend. (For interpretation of the references to color in this figure legend, the reader is referred to the web version of this article.)

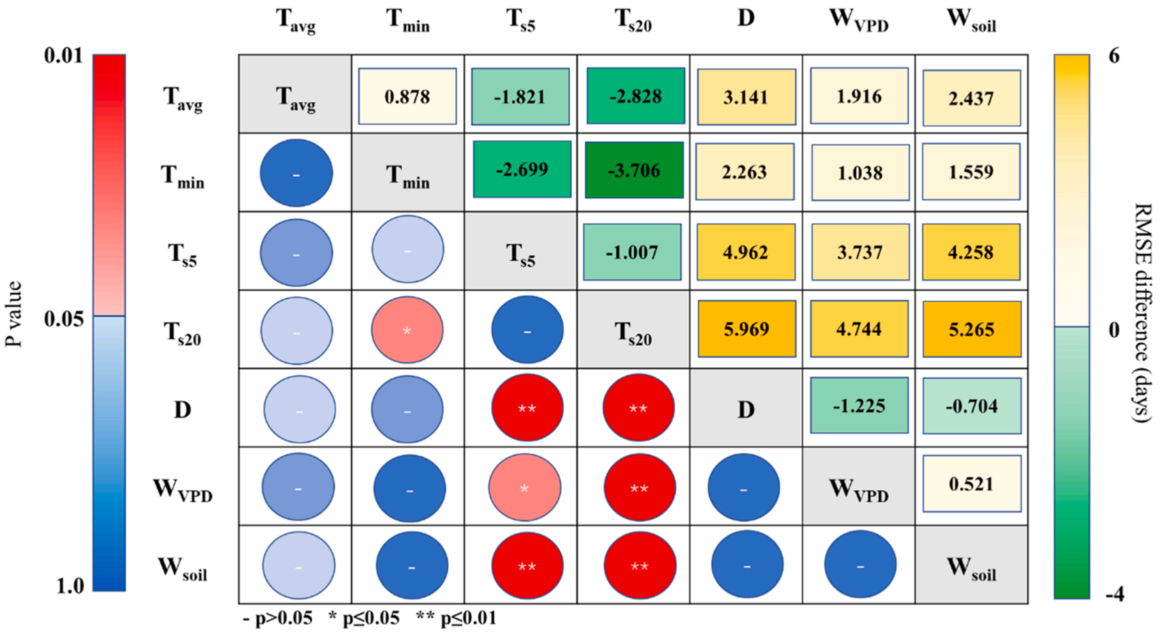

Fig. 4. Multiple comparison result of different factors. The bottom left region shows the P values from multiple group comparison tests for the RMSE of different factors. The top right region shows the RMSE difference between the column factor and the row factor.

RMSE of T_{s20} was more than 4.7 days lower than that due to daylength and water availability factors. Four out of six RMSE difference comparison groups between T_{s20} and most other factors (i.e., D, W_{VPD}, W_{soil} and T_{min}) passed the significance test at $\alpha = 0.05$, and groups between T_{s20} and D, W_{VPD}, W_{soil} even passed the significance test at $\alpha = 0.01$ (Fig. 4). The aforementioned results indicate that T_{s20} might be the most critical driving factor in determining rubber leaf senescence. T_{s5} also showed good performance with a slightly lower mean RMSE (7.7 days). All the RMSE difference comparison groups between T_{s5} and other non-temperature factors (i.e., W_{soil}, W_{VPD}, D) passed the significance test at $\alpha = 0.05$ (Fig. 4). It is worth noting that though the mean RMSE of T_{s5} and T_{s20} was about 1–3 days lower than that of T_{avg}, no significant differences were found between T_{avg}, T_{s5} and T_{s20}. D performed the worst as it had the largest mean RMSE (12.7 days). W_{soil} was marginally better than D with a mean RMSE of 12.0 days. No significant differences were found among D, W_{VPD} and W_{soil} (Fig. 4).

3.3. Performance of different models

Since non-temperature factors were found to not be the driving factors, comparison of different models was conducted based only on temperature factors. Comparison of RMSE of predicted leaf senescence date for each model using temperature factors shows that mean RMSEs of TTF, TTFs, SQF, SQFs, PAF, PAFs and ATF are all significantly lower than that for the null model (predicted as mean date of leaf senescence over all years) (Figs. 5 and 6), indicating that an overwhelming majority of models performed better than the null model. Though the gap of mean RMSE among TTF, TTFs, SQF, SQFs, PAF, PAFs and ATF can be as large as 2.6 days (Fig. 5), no significant differences are found among these models (Fig. 6). It can be observed that the mean RMSE of TTFs (6.6 days), SQFs (8.4 days) and PAFs (8.3 days) is around 1–2 days lower than that of TTF (8.5 days), SQF (8.8 days) and PAF (9.2 days), respectively (Fig. 5), indicating that models using sigmoid function in the pre-stress state performed slightly better than those not using sigmoid function. However, this difference is not significant (Fig. 6). It is worth noting that no significant differences were found between most models with pre-stress state (i.e., SQF, SQFs, PAFs, ATF) and without pre-stress state (TTF, TTFs) (Fig. 6). As unexpected, the UNF model did not show better performance when compared with other process-based models. On the contrary, the mean RMSE of the UNF model was about 1–4 days higher than that for all the other process-based models (Fig. 5). However, it still performed better than the null model (mean RMSE of 10.4 days in the UNF model compared with mean RMSE of 15.3 days in the null model). It is interesting that the mean RMSE of TTFs was the lowest (6.6 days) of all the models. Additionally, mean RMSE of TTFs is significantly lower than that of PAF, UNF and the null model (Fig. 6). Although TTFs has the lowest mean RMSE, it does not occupy the lowest RMSE when comparing all the models. Instead, SQFs had the lowest RMSE (5.5 days) when using T_{s20} as a driving factor.

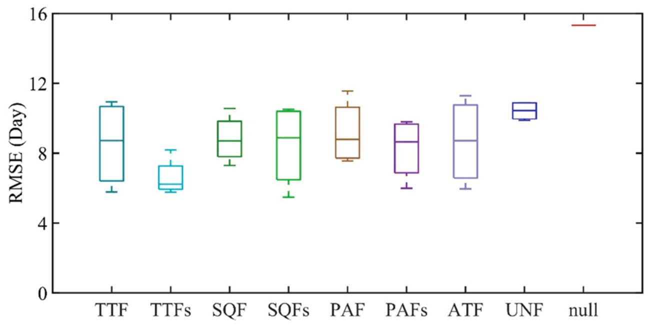

Fig. 5. Comparison of different models in predicting rubber leaf senescence.

3.4. Parameters of selected models and factors

Based on the performance of all models and factors, seven models (TTF, TTFs, SQF, SQFs, PAF, PAFs and ATF) and two factors (T_{avg} and T_{s20}) were selected to develop their models for rubber leaf senescence. The parameters of these models and factors are shown in Table 4. The start of baseline date (t_0) ranged from 52 (52 days since the initial date of September 23, namely November 13) to 107 (next January 7) in T_{avg}-based models and from 51 (November 12) to 73 (December 4) in T_{s20}-based models. Results show that t_0 of T_{avg}-based models was significantly later than that of T_{s20}-based models. For example, the mean date of t0 for T_{avg}-based models was 83 (December 14), which was 26 days later than that (November 19) for T_{s20}-based models. The much earlier response of T_{s20} than T_{avg} may indicate the longer cold temperature

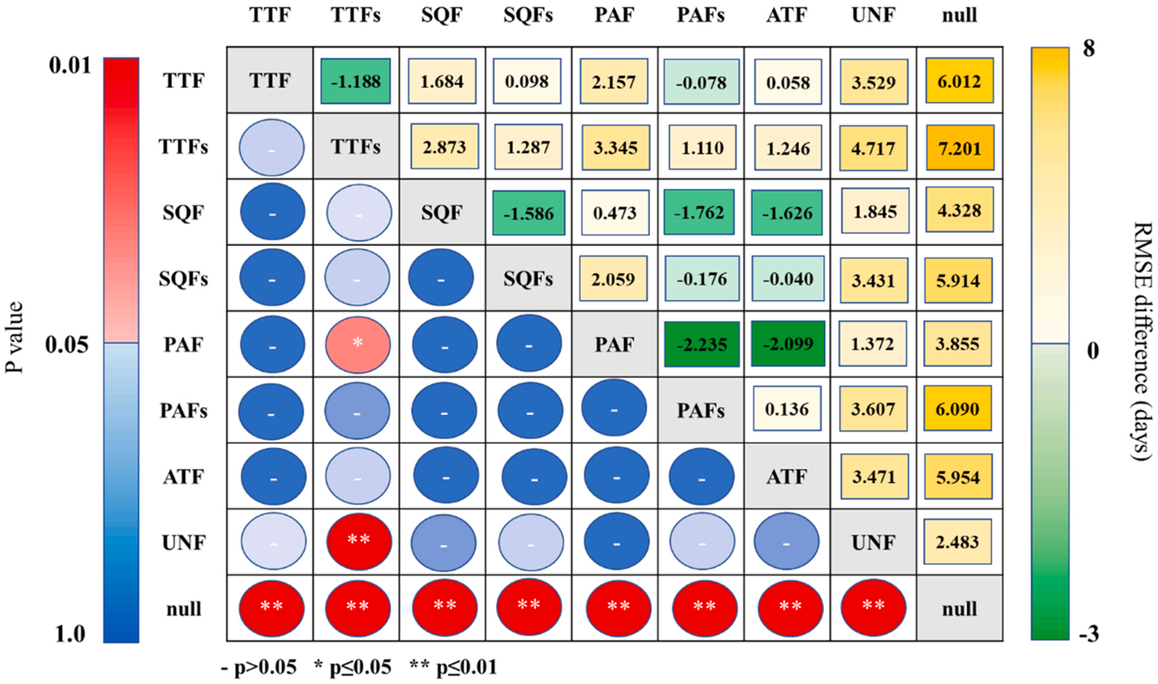

Fig. 6. Multiple comparison result of different models. The bottom left region shows the P values from multiple group comparison tests for the RMSE of different models. The top right region shows the RMSE difference between the column corresponding model and the row corresponding model.

Table 4
Parameter estimates of selected leaf senescence models for rubber plantations.

T_{avg}	TTF	TTFs	SQF	SQFs	PAF	PAFs	ATF
t_0	79	52	98	107	71	97	76
T_{base}	19.75		19.94	19.34	19.40	19.01	19.87
F_{crit}	-122.78	-47.00	-136.15	-266.06	-68.61	-27.33	
t_c			73	77	58	77	76
P_{req}			-1805.47	-1.59	-1223.30	-85.46	
T_{s20}	TTF	TTFs	SQF	SQFs	PAF	PAFs	ATF
t_0	52	54	73	55	52	63	51
T_{base}	26.71		24.91	25.98	23.33	26.01	27.16
F_{crit}	-298.12	-31.65	-190.06	-249.83	-24.07	-120.64	
t_c			44	52	30	53	51
P_{req}			-100.53	-66.96	-1273.33	-189.74	

Note: t_0, t_c, T_{base}, F_{crit} and P_{req} represent the start of baseline date, the start of pre-stress date, the baseline threshold of driving factor, the criteria for forcing state and the request of pre-stress units, respectively. The initial date (Day 1) starts from September 23.

accumulation period that soil temperature needs to reach a certain threshold than air temperature does. The start date of pre-stress (t_c) showed much lower variations among different T_{avg}-based models compared with t0. Mean date of t_c for T_{avg}-based models was 72 (December 4), which was 11 days earlier than the mean date of t_0. Unexpectedly, the mean date of tc for T_{s20}-based models was also 11 days earlier than its corresponding mean date of t_0.

The base temperature (T_{base}) had a very small variation among different T_{avg}-based models with a mean temperature of 19.55 °C. This implies that the air temperature threshold for rubber leaf senescence was possibly located between 19 °C and 20 °C. The base temperatures of T_{s20}-based models ranged from 23.33 °C to 27.16 °C and were much higher than the air temperature threshold. This is because the soil temperature of rubber forests generally had a higher value than air temperature. The forcing criteria (F_{crit}) varied largely for both T_{avg}-based models and T_{s20}-based models. For example, a low criteria of T_{avg} (−27.33 °C) was required for the PAFs model while a high criteria of T_{avg} (−266.06 °C) was required for the SQFs model. This is reasonable as algorithms of these models were various. Same large variations can also be found in the request of accumulated pre-stress units (P_{req}). As the accumulated pre-stress units based on the sigmoid function were much smaller than that using the trapezoid function, the P_{req} of SQF and PAF was much larger than that of SQFs and PAFs, respectively.

4. Discussion

4.1. Factors controlling rubber leaf senescence

The generally lower mean RMSE from temperature-based models than that from moisture indicated cold stress rather than soil or atmosphere drought stresses was the critical driving factor in rubber leaf senescence. This conclusion is consistent with the findings of Lin et al. (2018) who examined the relationship between observations of sap flow density and climatic factors. The finding of cold stress mainly driving rubber leaf senescence differs from some previous views (Chen et al., 2010; Guardiola-Claramonte et al., 2010; Liu et al., 2014) which suggested the importance of drought stress or the interaction of cold and drought stress in contributing to rubber leaf senescence. Due to the lack of phenological observations and corresponding abiotic data in other different latitudes within Asia tropics, we were unable to conduct direct model test. However, the conclusion of this study can be indirectly supported by the observed relationship between rubber defoliation duration and latitudes. Thus, we searched rubber defoliation duration records in Asian tropics from literatures. A total of seven study sites were found (Dong et al., 2013; Guardiola-Claramonte et al., 2008; Kumagai et al., 2015; Niu et al., 2017; Sopharat et al., 2015). Integration of the results from these studies demonstrated a strong correlation between rubber defoliation duration and the increase of latitude in Asian tropics (Fig. 7). It indicates that higher latitudes with lower temperatures had shorter defoliation durations, which is consistent with the finding of this study that low temperature controls the process of rubber leaf senescence.

Results of this study show RMSEs of soil temperature–based models were slightly lower than those for air temperature–based models. However, the RMSE difference was not significant. Since air temperature data is much easier to obtain from existing weather stations when compared with soil temperature data, we suggest the former would be the first choice to predict rubber leaf senescence.

Atmospheric drought or soil drought plays an uncritical role in driving rubber leaf senescence. This is not only because of the larger mean RMSE of these two climate factors (W_{soil} and W_{VPD}) when compared with temperature factors as reported in this study, it also can be inferred by some experimental observations which found that rubber trees exhibit deep roots and can absorb water from deep soil layers when soil drought happens (Guardiola-Claramonte et al., 2010; Liu et al., 2014). The rubber leaf requires more water for transpiration when atmospheric drought happens (a high value of VPD). This water deficit could be replenished by deep soil water in order to relieve leaf moisture stress which may result in leaf senescence. Daylength is usually regarded as an important factor in driving leaf senescence (Jolly et al., 2005; Piao et al., 2019; White et al., 1997). It can determine how much carbon dioxide could be fixed daily by leaf photosynthesis. Leaf coloring and fall is highly probable when the glucose produced by photosynthesis is not enough for its maintenance respiration. However, in this study, daylength was not found to be a controlling factor as it had the highest mean RMSE (12.7 days). Compared with other climatic factors, daylength is not a limited resource in tropical regions as its variation is relatively smaller compared with that in high latitude regions. Similar to our results, daylength was found to be not indispensable for some tree species in Austria, Germany and the United Kingdom where it becomes progressively shorter before leaf senescence (Olsson and Jonsson, 2015). The low influence of daylength on tree leaf senescence was also evidenced by Yue et al. (2015) who found, by probing the phenology trend of deciduous forests in the United States for the past 30 years, that including daylength did not improve model performance.

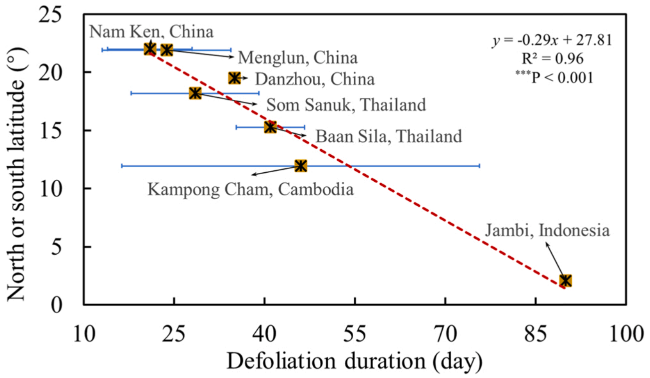

Fig. 7. Scatterplot between rubber defoliation duration and latitude in Asian tropics. The dashed red line represents the negative linear trend. The blue line segment represents the standard deviation of defoliation duration records. (For interpretation of the references to color in this figure legend, the reader is referred to the web version of this article.)

4.2. *Models for predicting rubber leaf senescence*

Unlike spring phenology models which have been extensively compared, the comparison of leaf senescence models has been barely investigated. This is mainly because current studies on leaf senescence are still limited (Piao et al., 2019). In the present study, the lower RMSEs of most models when compared with the null model implies the superior advantage of using process-based models. The relatively low mean RMSE indicates most process-based models are able to predict the rubber leaf senescence phenology. The comparison of 56 process-based models for rubber leaf senescence revealed a surprisingly small effect of model structure on the quality of prediction under the current climate. Besides, no significant difference between one-phase models (i.e., TTF, TTFs) and two-phase models (i.e., SQF, SQFs, PAF, PAFs, ATF and UNF) was found in this study. This result is consistent with the conclusion of spring models investigated by Yun et al. (2017). Though there is no evidence on which model performed best in terms of RMSE, using the simplest model should be the best choice considering its stronger operability and interpretability. Thus, we recommend the TTF model should be the first choice to predict rubber leaf senescence in this study as it is much easier to understand and operate compared with other process-based models.

RMSE comparison with similar species could evaluate the performance of our proposed rubber leaf senescence models from another aspect. However, there is barely any similar study on rubber leaf senescence modeling to date. Thus, comparing our results with leaf senescence of other species and spring models might be an alternative. The mean RMSE of rubber leaf senescence models ranged from 6 days to 8 days when using T_{s20} or T_{avg} as the driving factor, which is comparable with 8 days of mean RMSE of 27 woody and herbaceous species in the Qinghai–Tibetan Plateau (Lang et al., 2019), 10–13 days for three deciduous trees in France (Delpierre et al., 2009) and results of most spring phenology studies (Basler, 2016; Olsson and Jönsson, 2014; Xu and Chen, 2013; Zhao et al., 2021).

4.3. *Uncertainty and future directions*

One major uncertainty comes from lack of clarity regarding the rubber leaf senescence mechanism. Some previous phenology models applied decreasing degree-days (DDD) to simulate the response of leaf senescence based on either specific temperature or daylength thresholds (Delpierre et al., 2009; White et al., 1997). Fu et al. (2014) assumed leaf senescence starts to occur when the maximum carbohydrate storage capacity is reached. Lang et al. (2019) proposed an autumn leaf phenology model based on daily minimum temperature and daylength and assumed that plant leaf coloring is controlled by the interaction of low temperature and daylength and starts when either daylength or minimum temperature achieves a threshold. In this study, we proposed eight rubber leaf senescence models modified from traditional spring phenology models and found that most of them were able to predict rubber leaf senescence dates with RMSE ranging from 6 to 9 days. The forcing mechanism of these models is based on either DDD function or sigmoid function.

The limited phenological observations could introduce uncertainty in finalizing the rubber leaf senescence model. In fact, the beginning of recording year in China was generally later than that in European and North American countries, resulting in relatively shorter periods of phenology observations (Xu and Chen, 2013). In this study, rubber leaf senescence observations were recorded for only 19 years. In order to fully use the limited samples, we applied a 10 times leave-one-out cross-validation. This sampling strategy may reduce errors to a certain degree. Though the source of this uncertainty is clear, it is difficult to quantify the influence of limited records on the final result.

The importance of integrated and consistent records in investigating the mechanism of rubber leaf senescence and its response to climate change needs the reconstruction of long-term rubber leaf senescence datasets (Piao et al., 2019). As the history of remote sensing data such as Landsat images could be traced back to the middle of 1970 s, integrating satellite data with phenological observations is a promising method to construct long-term records. The high temporal resolution of MODIS dataset (twice per day) is another choice (Zhang et al., 2003). As there are different scales represented by remote sensing data and in situ observations, the key to reconstructing a consistent phenology dataset is to develop good temporal connections between them. As a point study has limitations in representing phenology at a vegetation community and landscape scale (Xu and Chen, 2013), upscaling point observation to a spatial scale is necessary. Thus, bridging the in situ records and satellite observations is another important research direction (Jeong and Medvigy, 2014; Zhang et al., 2017). Recent developments in near-surface instruments, such as phenology cameras and unmanned aerial vehicle (UAV), may provide some connections linking the in situ and satellite-observed phenology dates.

Although this study provided a new insight into the response of rubber leaf senescence to environmental factors, more research and experiments are needed to further clarify the mechanism of rubber leaf senescence. Combinations of multiple factors could be a possible direction. Experiments linking physiological traits and physical changes before, during and after rubber leaf senescence are also scarce. Besides, satellite-based sun-induced chlorophyll fluorescence (SIF) may provide opportunities for retrieving tropical forest phenology. SIF is a sensitive indicator in reflecting the canopy carbon and water exchanges (Yang et al., 2015) and has been applied to investigate the phenology of some tropical forest regions, such as the Amazon (Joiner et al., 2014; Jones et al., 2014).

5. Conclusion

In this study, we first investigated the driver of leaf senescence for introduced rubber trees which are originally evergreen in their traditional ranges. To examine the roles of temperature, daylength and water availability in driving rubber leaf senescence, we proposed a family of leaf senescence models: TTF, TTFs, SQF, SQFs, PAF, PAFs, ATF and UNF. Results show that low temperature was found to be the most critical driving factor. Both air temperature and soil temperature showed strong effects on rubber leaf senescence. Air temperature is recommended as the driver of choice due to its easy accessibility. Daylength and water availability showed significantly higher RMSEs than temperature. Thus, we suggest cold stress rather than soil or atmosphere drought stresses is a critical driving factor for rubber leaf senescence. The process-based models had a good ability to predict rubber leaf senescence dates. However, no significant differences were found among our proposed models and also between models with pre-stress or without pre-stress state. Considering its operability and interpretability, the TTF model is recommended as the first choice to predict rubber leaf senescence in this study as it is much easier to understand and operate compared with other process-based models. This study helps to better understand the driving mechanism of rubber leaf senescence. Future efforts should be directed towards integrating remotely sensed datasets and models, conducting experiments linking physiological traits and physical changes and developing more mechanism leaf senescence models.

CRediT authorship contribution statement

Yaoliang Chen: Conceptualization, Funding acquisition, Investigation, Methodology, Project administration, Software, Validation, Visualization, Writing – original draft. **Qinghai Song**: Conceptualization, Formal analysis, Investigation, Resources, Supervision, Writing – original draft. **Shusen Wang**: Conceptualization, Methodology, Supervision, Writing – original draft. **Ruiwu Zhou**: Investigation, Resources, Software, Validation. **Palingamoorthy Gnanamoorthy**: Methodology, Writing – original draft. **Houbing Chen**: Investigation, Software, visualization.

Declaration of Competing Interest

The authors declare that they have no known competing financial interests or personal relationships that could have appeared to influence the work reported in this paper.

Acknowledgments

This work was supported by the National Natural Science Foundation of China [grant number 41901124]; the open fund of CAS Key Laboratory of Tropical Forest Ecology, Xishuangbanna Tropical Botanical Garden, Chinese Academy of Sciences [grant number 20-CAS-TFE-01]. We thank to National Forest Ecosystem Research Station at Xishuangbanna for the data support.

References

Basler, D., 2016. Evaluating phenological models for the prediction of leaf-out dates in six temperate tree species across central Europe. Agric. For. Meteorol. 217, 10–21. https://doi.org/10.1016/j.agrformet.2015.11.007.

Basler, D., Koerner, C., 2014. Photoperiod and temperature responses of bud swelling and bud burst in four temperate forest tree species. Tree Physiol. 34, 377–388. https://doi.org/10.1093/treephys/tpu021.

Bréda, N., Huc, R., Granier, A., Dreyer, E., 2006. Temperate forest trees and stands under severe drought: a review of ecophysiological responses, adaptation processes and long-term consequences. Ann. For. Sci. 63. https://doi.org/10.1051/forest:2006042.

Broadhead, J.S., Ong, C.K., Black, C.R., 2003. Tree phenology and water availability in semi-arid agroforestry systems. For. Ecol. Manag. 180, 61–73. https://doi.org/10.1016/S0378-1127(02)00602-3.

Caffarra, A., Donnelly, A., Chuine, I., 2011. Modelling the timing of Betula pubescens budburst. II. Integrating complex effects of photoperiod into process-based models. Clim. Res. 46, 159–170. https://doi.org/10.3354/cr00983.

Cannell, M.G.R., Smith, R.I., 1983. Thermal time, chill days and prediction of budburst in Picea sitchensis. J. Appl. Ecol. 20, 951–963. https://doi.org/10.2307/2403139.

Carr, M.K.V., 2012. The water relations of rubber (Hevea brasiliensis): A review. Exp. Agric. 48, 176–193. https://doi.org/10.1017/S0014479710000645.

Chen, J.W., Cao, K.F., 2015. A possible link between hydraulic properties and leaf habits in Hevea brasiliensis. Funct. Plant Biol. 42, 718–726. https://doi.org/10.1071/FP14294.

Chen, J.W., Zhang, Q., Li, X.S., Cao, K.F., 2010. Gas exchange and hydraulics in seedlings of Hevea brasiliensis during water stress and recovery. Tree Physiol. 30, 876–885. https://doi.org/10.1093/treephys/tpq043.

Chuine, I., 2000. A unified model for budburst of trees. J. Theor. Biol. 207, 337–347. https://doi.org/10.1006/jtbi.2000.2178.

Chuine, I., 2010. Why does phenology drive species distribution? Philos. Trans. R. Soc. Biol. Sci. 365, 3149–3160. https://doi.org/10.1098/rstb.2010.0142.

Chuine, I., Cour, P., Rousseau, D.D., 1998. Fitting models predicting dates of flowering of temperate-zone trees using simulated annealing. Plant Cell Environ. 21, 455–466 https://dor.org/10.1046/j.1365-3040.1998.00299.x.

Cleland, E.E., Chuine, I., Menzel, A., Mooney, H.A., Schwartz, M.D., 2007. Shifting plant phenology in response to global change. Trends Ecol. Evol. 22, 357–365. https://doi.org/10.1016/j.tree.2007.04.003.

Cook, B.I., Wolkovich, E.M., Parmesan, C., 2012. Divergent responses to spring and winter warming drive community level flowering trends. Proc. Natl. Acad. Sci. 109, 9000–9005. https://doi.org/10.1073/pnas.1118364109.

Delpierre, N., Dufrene, E., Soudani, K., Ulrich, E., Cecchini, S., Boe, J., Francois, C., 2009. Modelling interannual and spatial variability of leaf senescence for three deciduous tree species in France. Agric. For. Meteorol. 149, 938–948. https://doi.org/10.1016/j.agrformet.2008.11.014.

Delpierre, N., Vitasse, Y., Chuine, I., Guillemot, J., Bazot, S., Rutishauser, T., Rathgeber, C.B.K., 2016. Temperate and boreal forest tree phenology: from organ-scale processes to terrestrial ecosystem models. Ann. For. Sci. 73, 5–25. https://doi.org/10.1007/s13595-015-0477-6.

Di Lucchio, L.M., Fensholt, R., Markussen, B., Raebild, A., 2018. Leaf phenology of thirteen African origins of baobab (Adansonia digitata (L.)) as influenced by daylength and water availability. Ecol. Evol. 8, 11261–11272. https://doi.org/10.1002/ece3.4600.

Dong, J., Xiao, X., Chen, B., Torbick, N., Jin, C., Zhang, G., Biradar, C., 2013. Mapping deciduous rubber plantations through integration of PALSAR and multi-temporal Landsat imagery. Remote Sens. Environ. 134, 392–402. https://doi.org/10.1016/j.rse.2013.03.014.

Dragoni, D., Schmid, H.P., Wayson, C.A., Potter, H., Grimmond, C.S.B., Randolph, J.C., 2011. Evidence of increased net ecosystem productivity associated with a longer vegetated season in a deciduous forest in south-central Indiana, USA. Glob. Change Biol. 17, 886–897. https://doi.org/10.1111/j.1365-2486.2010.02281.x.

Estrella, N., Menzel, A., 2006. Responses of leaf colouring in four deciduous tree species to climate and weather in Germany. Clim. Res. 32, 253–267. https://doi.org/10.3354/cr032253.

Fox, J., Castella, J.C., 2013. Expansion of rubber (Hevea brasiliensis) in Mainland Southeast Asia: what are the prospects for smallholders? J. Peasant Stud. 40, 155–170. https://doi.org/10.1080/03066150.2012.750605.

Fracheboud, Y., Luquez, V., Bjorken, L., Sjodin, A., Tuominen, H., Jansson, S., 2009. The control of autumn senescence in european aspen. Plant Physiol. 149, 1982–1991. https://doi.org/10.1104/pp.108.133249.

Fu, Y.H., Zhao, H., Piao, S., Peaucelle, M., Peng, S., Zhou, G., Ciais, P., Huang, M., Menzel, A., Uelas, J.P., Song, Y., Vitasse, Y., Zeng, Z., Janssens, I.A., 2015. Declining global warming effects on the phenology of spring leaf unfolding. Nature 526, 104. https://doi.org/10.1038/nature15402.

Fu, Y.S.H., Campioli, M., Vitasse, Y., De Boeck, H.J., Van den Berge, J., AbdElgawad, H., Asard, H., Piao, S., Deckmyn, G., Janssens, I.A., 2014. Variation in leaf flushing date influences autumnal senescence and next year's flushing date in two temperate tree species. Proc. Natl. Acad. Sci. 111, 7355–7360. https://doi.org/10.1073/pnas.1321727111.

Fu, Y.S.H., Zhang, X., Piao, S.L., Hao, F.H., Geng, X.J., Vitasse, Y., Zohner, C., Penuelas, J., Janssens, I.A., 2019. Daylength helps temperate deciduous trees to leaf-out at the optimal time. Glob. Change Biol. 25, 2410–2418. https://doi.org/10.1111/gcb.14633.

Ge, Q., Wang, H., Rutishauser, T., Dai, J., 2015. Phenological response to climate change in China: a meta-analysis. Glob. Change Biol. 21, 265–274. https://doi.org/10.1111/gcb.12648.

George, S., Suresh, P.R., Wahid, P.A., Nair, R.B., Punnoose, K.I., 2009. Active root distribution pattern of Hevea brasiliensis determined by radioassay of latex serum. Agrofor. Syst. 76, 275–281. https://doi.org/10.1007/s10457-008-9104-y.

Guardiola-Claramonte, M., Troch, P.A., Ziegler, A.D., Giambelluca, T.W., Durcik, M., Vogler, J.B., Nullet, M.A., 2010. Hydrologic effects of the expansion of rubber (Hevea brasiliensis) in a tropical catchment. Ecohydrology 3, 306–314. https://doi.org/10.1002/eco.110.

Guardiola-Claramonte, M., Troch, P., Ziegler, A., Giambelluca, T., Vogler, J., Nullet, M., 2008. Local hydrologic effects of introducing non-native vegetation in a tropical catchment. Ecohydrology 1, 13–22. https://doi.org/10.1002/eco.3.

Hänninen, H., 1990. Modelling bud dormancy release in trees from cool and temperate regions. Acta For. Fenn. 213.

Hanninen, H., 2016. Boreal and temperate trees in a changing climate (Biometeorology). Springer,, Dordrecht.

Hufkens, K., Basler, D., Milliman, T., Melaas, E.K., Richardson, A.D., 2018. An integrated phenology modelling framework in R. Methods Ecol. Evol. 9, 1276–1285. https://doi.org/10.1111/2041-210X.12970.

Jeong, S.J., Medvigy, D., 2014. Macroscale prediction of autumn leaf coloration throughout the continental United States. Glob. Ecol. Biogeogr. 23, 1245–1254. https://doi.org/10.1111/geb.12206.

Jeong, S.J., Medvigy, D., Shevliakova, E., Malyshev, S., 2012. Uncertainties in terrestrial carbon budgets related to spring phenology. J. Geophys. Res. -Biogeosciences 117. https://doi.org/10.1029/2011JG001868.

Joiner, J., Yoshida, Y., Vasilkov, A., Schaefer, K., Jung, M., Guanter, L., Zhang, Y., Garrity, S., Middleton, E.M., Huemmrich, K.F., Gu, L., Marchesini, L.B., 2014. The seasonal cycle of satellite chlorophyll fluorescence observations and its relationship to vegetation phenology and ecosystem atmosphere carbon exchange. Remote Sens. Environ. 152, 375–391. https://doi.org/10.1016/j.rse.2014.06.022.

Jolly, W.M., Nemani, R., Running, S.W., 2005. A generalized, bioclimatic index to predict foliar phenology in response to climate. Glob. Change Biol. 11, 619–632. https://doi.org/10.1111/j.1365-2486.2005.00930.x.

Jones, M.O., Kimball, J.S., Nemani, R.R., 2014. Asynchronous Amazon forest canopy phenology indicates adaptation to both water and light availability. Environ. Res. Lett. 9. https://doi.org/10.1088/1748-9326/9/12/124021.

Kazan, K., 2015. Diverse roles of jasmonates and ethylene in abiotic stress tolerance. Trends Plant Sci. 20, 219–229. https://doi.org/10.1016/j.tplants.2015.02.001.

Keenan, T.F., Richardson, A.D., 2015. The timing of autumn senescence is affected by the timing of spring phenology: implications for predictive models. Glob. Change Biol. 21, 2634–2641. https://doi.org/10.1111/gcb.12890.

Keskitalo, J., Bergquist, G., Gardestrom, P., Jansson, S., 2005. A cellular timetable of autumn senescence. Plant Physiol. 139, 1635–1648. https://doi.org/10.1104/pp.105.066845.

Klosterman, S.T., Hufkens, K., Gray, J.M., Melaas, E., Sonnentag, O., Lavine, I., Mitchell, L., Norman, R., Friedl, M.A., Richardson, A.D., 2014. Evaluating remote sensing of deciduous forest phenology at multiple spatial scales using PhenoCam imagery. Biogeosciences 11, 4305–4320. https://doi.org/10.5194/bg-11-4305-2014.

Körner, C., Basler, D., 2010. Phenology under global warming. Science 327, 1461–1462. https://doi.org/10.1126/science.1186473.

Koyama, T., 2014. The roles of ethylene and transcription factors in the regulation of onset of leaf senescence. Front. Plant Sci. 5. https://doi.org/10.3389/fpls.2014.00650.

Kramer, P.J., 1940. Root resistance as a cause of decreased water absorption by plants at low temperatures. Plant Physiol. 15, 63–79. https://doi.org/10.1104/pp.15.1.63.

Kumagai, T., Mudd, R., Giambelluca, T., Kobayashi, N., Miyazawa, Y., Lim, T., Liu, W., Huang, M., Fox, J., Ziegler, A., 2015. How do rubber (Hevea brasiliensis) plantations behave under seasonal water stress in northeastern Thailand and central Cambodia? Agric. For. Meteorol. 213, 10–22. https://doi.org/10.1016/j.agrformet.2015.06.011.

Landsberg, J.J., 1974. Apple fruit bud development and growth: analysis and an Empirical Model. Ann. Bot. 38, 1013–1023.

Lang, G.A., 1987. Dormancy: a new universal terminology. Hortscience 22, 817–820.

Lang, W., Chen, X., Qian, S., Liu, G., Piao, S., 2019. A new process-based model for predicting autumn phenology: How is leaf senescence controlled by photoperiod and temperature coupling? Agric. For. Meteorol. 268, 124–135. https://doi.org/10.1016/j.agrformet.2019.01.006.

Lee, J.H., Park, Y.J., Kim, J.Y., Park, C.M., 2021. Phytochrome B conveys low ambient temperature cues to the Ethylene-Mediated leaf senescence in Arabidopsis. Plant Cell Physiol. 00, 1–14. https://doi.org/10.1093/pcp/pcab178.

Li, Y., Lan, G., Xia, Y., 2016. Rubber trees demonstrate a clear retranslocation under seasonal drought and cold stresses. Front. Plant Sci. 7, 1907. https://doi.org/10.3389/fpls.2016.01907.

Lin, Y., Zhang, Y., Zhao, W., Dong, Y., Fei, X., Song, Q., Sha, L., Wang, S., Grace, J., 2018. Pattern and driving factor of intense defoliation of rubber plantations in SW China. Ecol. Indic. 94, 104–116. https://doi.org/10.1016/j.ecolind.2018.06.050.

Liu, W., Li, J., Lu, H., Wang, P., Luo, Q., Liu, W., Li, H., 2014. Vertical patterns of soil water acquisition by non-native rubber trees (Hevea brasiliensis) in Xishuangbanna, southwest China. Ecohydrology 7, 1234–1244. https://doi.org/10.1002/eco.1456.

Liu, X., Jiang, L., Feng, Z., Li, P., 2016. Rubber plantation expansion related land use change along the Laos-China border region. Sustainability 8, 1011. https://doi.org/10.3390/su8101011.

Lürssen, K., 1991. Ethylene and agriculture. In: Mattoo, A., Suttle, J. (Eds.), The Plant Hormone Ethylene. CRC Press, Boca Raton, p. 12.

Mendez-Alonzo, R., Pineda-Garcia, F., Paz, H., Rosell, J.A., Olson, M.E., 2013. Leaf phenology is associated with soil water availability and xylem traits in a tropical dry forest. Trees-Struct. Funct. 27, 745–754. https://doi.org/10.1007/s00468-012-0829-x.

Menzel, A., Sparks, T.H., Estrella, N., Koch, E., Aasa, A., Ahas, R., Alm-Kuebler, K., Bissolli, P., Braslavska, Og, Briede, A., Chmielewski, F.M., Crepinsek, Z., Curnel, Y., Dahl, A., Defila, C., Donnelly, A., Filella, Y., Jatcza, K., Mage, F., Mestre, A., Nordli, O., Penuelas, J., Pirinen, P., Remisova, V., Scheifinger, H., Striz, M., Susnik, A., Van Vliet, A.J.H., Wielgolaski, F.-E., Zach, S., Zust, A., 2006. European phenological response to climate change matches the warming pattern. Glob. Change Biol. 12, 1969–1976. https://doi.org/10.1111/j.1365-2486.2006.01193.x.

Migliavacca, M., Sonnentag, O., Keenan, T.F., Cescatti, A., O'Keefe, J., Richardson, A.D., 2012. On the uncertainty of phenological responses to climate change, and implications for a terrestrial biosphere model. Biogeosciences 9, 2063–2083. https://doi.org/10.5194/bg-9-2063-2012.

Niu, F., Röll, A., Meijide, A., Hölscher, D., 2017. Rubber tree transpiration in the lowlands of Sumatra. Ecohydrology 10, e1882. https://doi.org/10.1002/eco.1882.

Olsson, C., Jönsson, A.M., 2014. Process-based models not always better than empirical models for simulating budburst of Norway spruce and birch in Europe. Glob. Change Biol. 20. https://doi.org/10.1111/gcb.12593.

Olsson, C., Jonsson, A.M., 2015. A model framework for tree leaf colouring in Europe. Ecol. Model. 316, 41–51. https://doi.org/10.1016/j.ecolmodel.2015.08.002.

Piao, S.L., Fang, J.Y., Zhou, L.M., Ciais, P., Zhu, B., 2006. Variations in satellite-derived phenology in China's temperate vegetation. Glob. Change Biol. 12, 672–685. https://doi.org/10.1111/j.1365-2486.2006.01123.x.

Piao, S.L., Liu, Q., Chen, A.P., Janssens, I.A., Fu, Y.S., Dai, J.H., Liu, L.L., Lian, X., Shen, M.G., Zhu, X.L., 2019. Plant phenology and global climate change: current progresses and challenges. Glob. Change Biol. 25, 1922–1940. https://doi.org/10.1111/gcb.14619.

Picornell, A., Buters, J., Rojo, J., Traidl-Hoffmann, C., Damialis, A., Menzel, A., Bergmann, K.C., Werchan, M., Schmidt-Weber, C., Oteros, J., 2019. Predicting the start, peak and end of the Betula pollen season in Bavaria, Germany. Sci. Total Environ. 690, 1299–1309. https://doi.org/10.1016/j.scitotenv.2019.06.485.

Priyadarshan, P.M., 2017. Biology of Hevea Rubber. Springer,, Switzerland.

Recio, M., Picornell, A., Trigo, M.M., Gharbi, D., Garcia-Sanchez, J., Cabezudo, B., 2018. Intensity and temporality of airborne Quercus pollen in the southwest Mediterranean area: Correlation with meteorological and phenoclimatic variables, trends and possible adaptation to climate change. Agric. For. Meteorol. 250, 308–318. https://doi.org/10.1016/j.agrformet.2017.11.028.

Richardson, A.D., Keenan, T.F., Migliavacca, M., Ryu, Y., Sonnentag, O., Toomey, M., 2013. Climate change, phenology, and phenological control of vegetation feedbacks to the climate system. Agric. For. Meteorol. 169, 156–173. https://doi.org/10.1016/j.agrformet.2012.09.012.

Ryan, C.M., Williams, M., Grace, J., Woollen, E., Lehmann, C.E.R., 2017. Pre- rain green-up is ubiquitous across southern tropical Africa: implications for temporal niche separation and model representation. N. Phytol. 213, 625–633. https://doi.org/10.1111/nph.14262.

Seghieri, J., Carreau, J., Boulain, N., De Rosnay, P., Arjounin, M., Timouk, F., 2012. Is water availability really the main environmental factor controlling the phenology of woody vegetation in the central Sahel? Plant Ecol. 213, 861–870. https://doi.org/10.1007/s11258-012-0048-y.

Semerci, A., Guevara, C.A., Gonzalez-Benecke, C.A., 2020. Water availability effects on growth and phenology of 11 poplar cultivars growing in semiarid areas in Turkey. N. For. https://doi.org/10.1007/s11056-020-09802-5.

Sopharat, J., Gay, F., Thaler, P., Sdoodee, S., Ayutthaya, S., Tanavud, C., Hammecker, C., Do, F., 2015. A simple framework to analyze water constraints on seasonal transpiration in rubber tree (Hevea brasiliensis) plantations. Front. Plant Sci. 5. https://doi.org/10.3389/fpls.2014.00753.

Tian, F., Wigneron, J.P., Ciais, P., Chave, J., Ogee, J., Penuelas, J., Raebild, A., Domec, J.-C., Tong, X., Brandt, M., Mialon, A., Rodriguez-Fernandez, N., Tagesson, T., Al-Yaari, A., Kerr, Y., Chen, C., Myneni, R.B., Zhang, W., Ardo, J., Fensholt, R., 2018. Coupling of ecosystem-scale plant water storage and leaf phenology observed by satellite. Nat. Ecol. Evol. 2, 1428–1435. https://doi.org/10.1038/s41559-018-0630-3.

Wan, M., Liu, X., 1979. China's National Phenological Observational Criterion. Science press, Beijing.

Way, D.A., Montgomery, R.A., 2015. Photoperiod constraints on tree phenology, performance and migration in a warming world. Plant Cell Environ. 38, 1725–1736. https://doi.org/10.1111/pce.12431.

White, M.A., Thornton, P.E., Running, S.W., 1997. A continental phenology model for monitoring vegetation responses to interannual climatic variability. Glob. Biogeochem. Cycles 11. https://doi.org/10.1029/97GB00330.

Wu, C., Wang, J., Ciais, P., Penuelas, J., Zhang, X., Sonnentag, O., Tian, F., Wang, X., Wang, H., Liu, R., Fu, Y.H., Ge, Q., 2021. Widespread decline in winds delayed autumn foliar senescence over high latitudes. Proc. Natl. Acad. Sci. USA 118. https://doi.org/10.1073/pnas.2015821118.

Xu, L., Chen, X., 2013. Regional unified model-based leaf unfolding prediction from 1960 to 2009 across northern China. Glob. Change Biol. 19, 1275–1284. https://doi.org/10.1111/gcb.12095.

Yang, X., Tang, J., Mustard, J.F., Lee, J.E., Rossini, M., Joiner, J., Munger, J.W., Kornfeld, A., Richardson, A.D., 2015. Solar-induced chlorophyll fluorescence that correlates with canopy photosynthesis on diurnal and seasonal scales in a temperate deciduous forest. Geophys. Res. Lett. 42, 2977–2987. https://doi.org/10.1002/2015GL063201.

Yue, X., Unger, N., Keenan, T.F., Zhang, X., Vogel, C.S., 2015. Probing the past 30-year phenology trend of US deciduous forests. Biogeosciences 12, 4693–4709. https://doi.org/10.5194/bg-12-4693-2015.

Yun, K., Hsiao, J., Jung, M.-P., Choi, I.-T., Glenn, D.M., Shim, K.-M., Kim, S.-H., 2017. Can a multi-model ensemble improve phenology predictions for climate change studies? Ecol. Model. 362, 54–64. https://doi.org/10.1016/j.ecolmodel.2017.08.003.

Zhang, X.Y., Friedl, M.A., Schaaf, C.B., Strahler, A.H., Hodges, J.C.F., Gao, F., Reed, B.C., Huete, A., 2003. Monitoring vegetation phenology using MODIS. Remote Sens. Environ. 84, 471–475. https://doi.org/10.1016/S0034-4257(02)00135-9.

Zhang, X., Wang, J., Gao, F., Liu, Y., Schaaf, C., Friedl, M., Yu, Y., Jayavelu, S., Gray, J., Liu, L., Yan, D., Henebry, G.M., 2017. Exploration of scaling effects on coarse resolution land surface phenology. Remote Sens. Environ. 190, 318–330. https://doi.org/10.1016/j.rse.2017.01.001.

Zhao, H., Fu, Y.H., Wang, X., Zhang, Y., Liu, Y., Janssens, I.A., 2021. Diverging models introduce large uncertainty in future climate warming impact on spring phenology of temperate deciduous trees. Sci. Total Environ. 757. https://doi.org/10.1016/j.scitotenv.2020.143903.

Zhao, M., Liu, W., Xia, X., Wang, T., Zhang, W.H., 2014. Cold acclimation-induced freezing tolerance of Medicago truncatula seedlings is negatively regulated by ethylene. Physiol. Plant. 152, 115–129. https://doi.org/10.1111/ppl.12161.